

Heat Capacity for the Binary System of Silybin and Sodium Cholate

Yuan-Yuan Wang, Yu-Li Li, Tong-Chun Bai,* and Miao Zhang

College of Chemistry, Chemical Engineering and Materials Science, Soochow University, Suzhou, 215123, China

ABSTRACT: The heat capacity (C_p) of solid mixtures of silybin and sodium cholate was measured by a differential scanning calorimeter (DSC). X-ray diffraction and the FT-IR spectroscopy were used to determine the structure of solid mixture. Our results indicate that this binary system is composed of a mixture of two microcrystalline structures. The transformation of heat capacity from silybin to sodium cholate passes through a minimum at $w_1 = 0.25$, where w_1 is the mass fraction of sodium cholate. Polynomial equations of heat capacity versus temperature and the virial equation of excess heat capacity versus composition were applied to correlate experimental data. The changes of thermodynamic functions of enthalpy, entropy, and Gibbs function were calculated from the data of C_p .

INTRODUCTION

Silybin is an antihepatotoxic polyphenolic substance isolated from the milk thistle plant, *Silybum marianum*. Its structure is shown in Figure 1. It is widely used as a drug to maintain liver health and to treat a range of liver and gallbladder disorders, including hepatitis, cirrhosis, and jaundice.^{1–3} The poor solubility in water limits its biological and medicinal application. To improve the solubility and to enhance the bioavailability of silybin, a variety of methods have been developed, among them including methods to incorporate silybin in a dosage form using liposomes,⁴ solid dispersions,⁵ and mixed micelles.⁶

Sodium cholate is one bile salt with the chemical structure shown in Figure 2. The ability of bile salts to enhance the oral bioavailability of poorly water-soluble drugs has been recognized for many years.^{7–10} Their micellar form and their mixture with lecithin as a drug carrier have gained much attention in pharmaceutical applications.^{6,7} It is reported that sodium cholate has been used to improve the bioavailability of silybin.⁶ In the processes of dosage formation, two steps are more important. One is the formation of a solid film of silybin-loaded sodium cholate/phospholipid-mixed micelles, which was prepared by a dispersion method. Another is the formation of a powder dosage of the mixed micelles, which was obtained by freeze-drying method. In these processes, the solid mixing state in the film and in the dosage powder is the key factor. The relevant information of solid mixing and the phase diagram are the basis of the technique.^{6,7}

Although numerous strategies exist for enhancing the bioavailability of hydrophobic drugs, the success of these approaches cannot be guaranteed, and it is greatly dependent on the physical and chemical nature of the molecules being developed. Crystal engineering offers a number of routes to improve solubility and dissolution rates that can be adopted through an in-depth knowledge of crystallization processes and the molecular properties of active pharmaceutical ingredients.¹¹ To address these problems, the physical chemical properties of pharmaceutical ingredients must be known in detail. Among many physical properties, heat capacity is an essential property when studying phase transitions, critical phenomena, and glass transitions.^{11–14} Therefore, it is an important property in the evaluation of the efficiency of drugs.

In solid mixtures, the drug may be present as the fully crystalline, fully amorphous or partially crystalline, partially amorphous state. The solubility and the release rate of the drug are seriously dependent on the solid state and also on sample composition.¹¹ In this work, the mixtures of silybin and sodium cholate were prepared by a solvent evaporation method. The heat capacity (C_p) of this binary system was measured by differential scanning calorimetry (DSC). By analyzing the effect of composition on C_p , information about phase transformations and the interactions between the two species can be obtained.

EXPERIMENTAL SECTION

Materials. Silybin (CAS. No. 22888-70-6, with IUPAC name 3,5,7-trihydroxy-2-[3-(4-hydroxy-3-methoxyphenyl)-2-hydroxymethyl-2,3-dihydrobenzo-[1,4]-dioxin-6-yl]-chroman-4-one) was purchased from Panjin Green Biological Development Co. Ltd., Liaoning, China. Its purity was 0.97 mass fraction determined by UV spectrometry at (252 to 288) nm. This purity was confirmed by high-performance liquid chromatography (HPLC); 96.8 % silybin, 1.1 % isosilybin, 0.8 % silydianin, 0.1 % silychristin, and 1.2 % other impurities. Sodium cholate (CAS. No.: 316-09-1, with IUPAC name sodium (4R)-4-[(3R,5S,7R,8R,9S,10S,12S,13R,14S,17R)-3,7,12-trihydroxy-10,13-dimethyl-2,3,4,5,6,7,8,9,11,12,14,15,16,17-tetradecahydro-1H-cyclopenta[*a*]phenanthren-17-yl] pentanoate) with a 0.990 mass fraction purity was obtained from SinoPharm Chemical Reagents Co. Ltd. The main impurity in sodium cholate is water. All samples were dried under vacuum at 333 K for 48 h before use.

Sample Preparation. The freshly dried compound was quickly weighed using a glass bottle with a hermetic seal cover. Accurately weighed silybin and sodium cholate were mixed to form binary mixtures. The composition of this mixture is determined at this step. For samples used in this work, the mass

Received: May 3, 2011

Accepted: June 28, 2011

Published: July 13, 2011

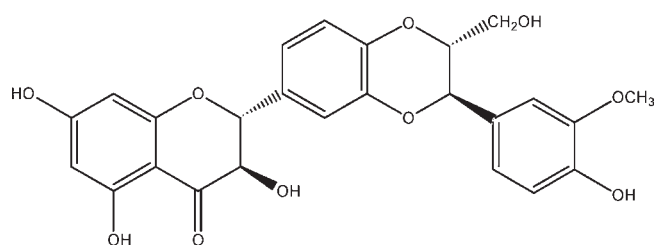


Figure 1. Chemical structures of silybin. CAS No.: 22888-70-6. IUPAC name: 3,5,7-trihydroxy-2-[3-(4-hydroxy-3-methoxyphenyl)-2-hydroxy-methyl-2,3-dihydrobenzo-[1,4]-dioxin-6-yl]-chroman-4-one.

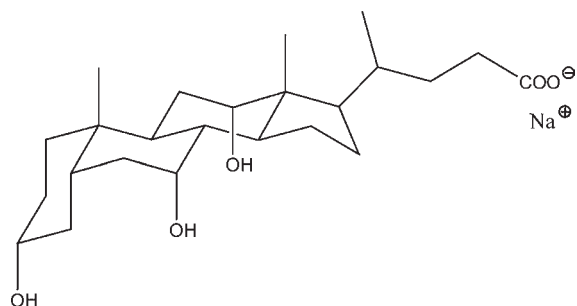


Figure 2. Molecular structure of sodium cholate. CAS No.: 316-09-1. IUPAC name: sodium (4R)-4-[(3R,5S,7R,8R,9S,10S,12S,13R,14S,17R)-3,7,12-trihydroxy-10,13-dimethyl-2,3,4,5,6,7,8,9,11,12,14,15,16,17-tetradecahydro-1H-cyclopenta[a]phenanthren-17-yl]pentanoate.

fractions of sodium cholate, w_1 , are (0.100, 0.200, 0.250, 0.333, 0.500, 0.667, 0.750, 0.801, and 0.900), respectively.

To mix the component completely, silybin was dissolved in ethanol, and sodium cholate was dissolved in water; then the two solutions were mixed together. Solvent evaporation was performed under reduced pressure at about 313 K in a rotary evaporator. After that, samples were dried further in a vacuum drying chamber under vacuum at 333 K for over 48 h and then stored over P_2O_5 in a desiccator before use. During these processes, solvent was added and then removed, but the mass ratio of the two components, silybin to sodium cholate, remained unchangeable.

DSC Analysis and Heat Capacity Measurements. The heat capacity was measured with a differential scanning calorimeter DSC (NETSCH, DSC-204F1, Germany). Certified indium wire encapsulated in an aluminum crucible was used for temperature and heat flow calibration. An empty aluminum pan and lid was used as the reference for all measurements. Nitrogen gas with a purity of 0.99999 (volume fraction) was used as a purge gas at a rate of $20 \text{ mL} \cdot \text{min}^{-1}$ and as a protective gas at $70 \text{ mL} \cdot \text{min}^{-1}$ during loading. Samples of about 5 mg were weighed to $\pm 0.01 \text{ mg}$ using a balance (model BT25S, Sartorius AG, Beijing). A thin disk of sapphire was used as the heat capacity standard.

The measurement of heat capacity includes three runs.^{14,15} An empty Al pan with a lid was the first run to obtain the baseline. The second and third runs were performed on the sapphire and the sample, respectively. One empty Al pan was used through three runs. A three-segment heating program was used in DSC operation. The first segment lasting for 15 min was an isothermal one at the initial temperature; the second segment was a dynamic one with a heating rate of $5 \text{ K} \cdot \text{min}^{-1}$, and the final segment

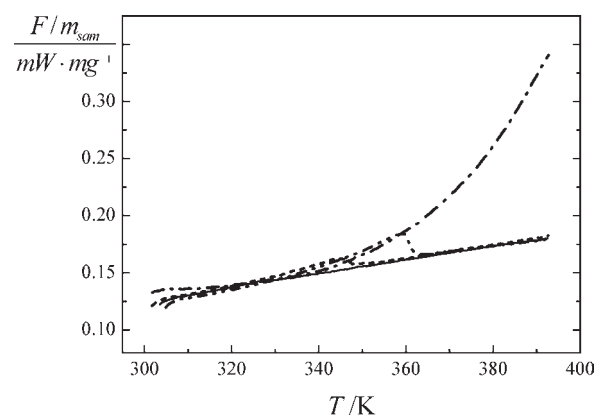


Figure 3. Four successive repeated DSC scans to sodium cholate, temperature range from (300 to 393) K, heating rate $2 \text{ K} \cdot \text{min}^{-1}$, under the protection of nitrogen gas. The sample loading mass is about 5 mg. The first scan (dash dot line) shows that water is evaporated; the second (dash dot dotted line) and third (short dashed line) scans show that the water content has been depressed significantly, and the fourth scan (solid line) shows that water has been evaporated perfectly. The mass loss during the fourth scans is confirmed to be 0.2 %.

lasting for 15 min was another isothermal one at the final temperature. The heat capacity is calculated by eq 1.

$$C_{p,\text{sam}} = C_{p,\text{std}} \frac{(F_{\text{sam}} - F_{\text{bsl}})m_{\text{std}}}{(F_{\text{std}} - F_{\text{bsl}})m_{\text{sam}}} \quad (1)$$

where $C_{p,\text{sam}}/\text{J} \cdot \text{K}^{-1} \cdot \text{g}^{-1}$ and $C_{p,\text{std}}/\text{J} \cdot \text{K}^{-1} \cdot \text{g}^{-1}$ are the heat capacity of the sample and standard substance (sapphire), respectively. F_{sam} , F_{bsl} , and F_{std} are the heat flows of the sample, baseline, and sapphire runs, respectively, and m_{std} and m_{sam} are the masses of the standard substance and the sample, respectively.

Thermogravimetric Analysis. Thermogravimetric (TG) analysis was used to determine the mass loss during the process of temperature programming. The TG experiment was performed with a TA Instruments SDT 2960 in a dynamic flow of nitrogen (0.99999 volume fraction). The gas flow rate was $100 \text{ mL} \cdot \text{min}^{-1}$. Approximately 5 mg of sample was weighed in an aluminum pan and heated at a rate of $10 \text{ K} \cdot \text{min}^{-1}$, and the loss of weight was recorded.

Infrared Spectroscopy. Fourier transform infrared (FT-IR) spectra were obtained on a Magna 550 FT-IR system (Nicolet) with the KBr disk method. The scanning range was (400 to 4000) cm^{-1} , and the resolution was 2 cm^{-1} .

X-ray Powder Diffraction. An X-ray powder diffraction (XRD) investigation was performed with a diffractometer (model: X'Pert PRO MPD, PANalytical Company, Holland): Cu-K α , $\lambda = 0.15406 \text{ nm}$, voltage: 40 kV, and 40 mA, with the angular range of $5 < 2\theta < 60^\circ$ in a step scan mode (step width 0.03).

RESULTS AND DISCUSSION

Thermal Analysis of Pure Sodium Cholate and Silybin. To set up the experimental steps and operating conditions to measure heat capacity, the thermal behavior of pure sodium cholate and silybin were analyzed first.

The TG test for silybin shows a mass loss due to water evaporation in temperature range below 413 K, but this mass loss is very small. If the sample was dried carefully, it was too

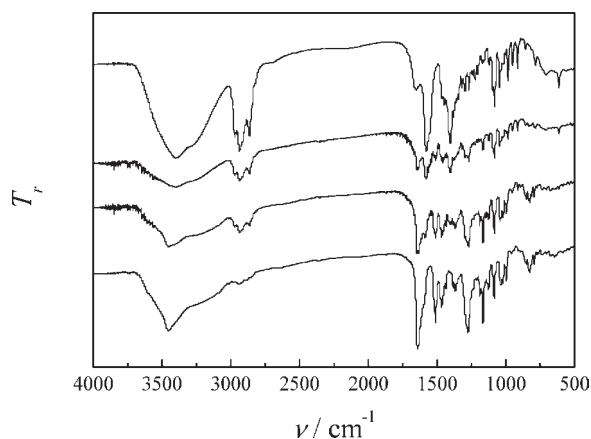


Figure 4. FT-IR spectra (transmittance T_r vs wavenumber ν) for mixtures of [sodium cholate (1) + silybin (2)] with mass fractions of $w_1 = (1, 0.801, 0.333, \text{ and } 0)$, in order from top to bottom.

small to be detected. Decomposition of silybin is found above 540 K. The DSC curve of silybin shows an endothermic peak due to the melting of solid silybin with a peak at 435.2 K and an exothermic peak due to the molecular decomposition at 540.4 K.

In the case of sodium cholate, water evaporation was found below 413 K, and the molecule decomposition was not observed in the temperature region below 453 K. If sample was dried carefully, the mass loss due to water evaporation could be reduced to less than 2 %.

On the basis of these observations, to measure the heat capacity for mixtures of silybin + sodium cholate by DSC, the temperature program should be operated below 373 K to avoid silybin melting, and the effect of water evaporation should be taken into consideration.

In this work, all samples were dried under vacuum at 333 K for 48 h before the DSC test. However, during the process of weighing the sample and loading into the crucibles, moisture was absorbed by the samples because of the hygroscopicity of the solids, especially for sodium cholate. To remove the water completely, the DSC scan was performed under the protection of nitrogen gas within the interval when the sample was loaded into the DSC instrument and prior to the C_p measurement. Figure 3 shows the DSC curves of pure sodium cholate in four successive repeated scans. The moisture has been removed satisfactorily after three repeated scans. By checking the sample mass before and after the fourth run, it was confirmed that the mass loss is less than 0.2 %. Comparatively, it is easier to remove moisture from silybin than from sodium cholate, that is to say that three repeated DSC scans is enough to remove water from silybin. Therefore, we set the three repeated DSC scans below 393 K as a program to remove water. The C_p was measured during the fourth run. To calculate the specific heat capacity, the sample mass weighed after the fourth run is used.

FT-IR Spectroscopy. Infrared spectra were recorded to determine if there were possible interactions and chemical reactions between silybin and sodium cholate in the solid mixtures. The infrared spectra of silybin, sodium cholate, and some of their mixtures ($w_1 = 0.333$ and 0.801) are shown in Figure 4.

For silybin the band at 3450 cm^{-1} is assigned to free $-\text{OH}$ bond vibration, 1640 cm^{-1} is assigned to the stretching vibration of the $\text{C}=\text{O}$ group, 1500 cm^{-1} is assigned to the aromatic group; 1270 cm^{-1} is assigned to the $=\text{C}-\text{O}-\text{C}$ vibration.¹⁶

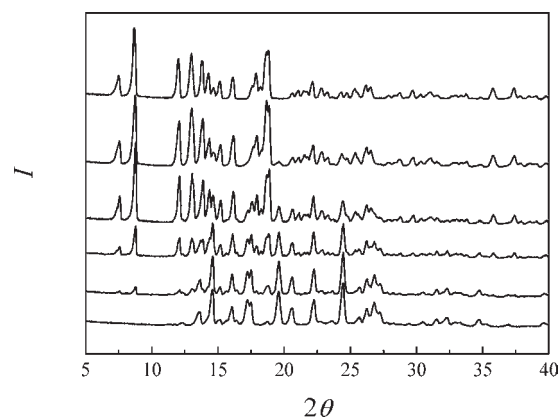


Figure 5. X-ray diffraction patterns (diffraction peak intensity I appearing at angles of 2θ) for mixtures of [sodium cholate (1) + silybin (2)] with mass fractions of $w_1 = (1, 0.900, 0.667, 0.333, 0.100, \text{ and } 0)$, in order from top to bottom.

The spectrum of sodium cholate shows that the band at 3400 cm^{-1} is attributed to the $\text{O}-\text{H}$ band. The bands around 2900 cm^{-1} are assigned to the vibration of $\text{O}-\text{H}$ and $\text{C}-\text{H}$ groups, which are characteristic of sodium cholate. The band at 1575 cm^{-1} is attributed to the vibration band of $\text{C}=\text{O}$ group, 1400 cm^{-1} is assigned to the CH_2 group, and 1080 cm^{-1} is assigned to the stretching vibration of $\text{C}-\text{O}$ band.¹⁶

The strength of the bands of silybin ($1640, 1500, \text{ and } 1270$) decreased with the increase in w_1 , whereas the bands of the sodium cholate ($2900, 1575, 1400, \text{ and } 1080 \text{ cm}^{-1}$) decreased with the increase in w_1 , and no band shift is observed. This trend is characteristic of a mixture, and no chemical interaction is evident between the two species.

X-ray Powder Diffraction. XRD gives information about the effect of the degree of crystallinity on the solid state. Figure 5 shows the XRD patterns of sodium cholate, silybin, and their mixtures with $w_1 = (0.900, 0.667, 0.333, \text{ and } 0.100)$. For pure sodium cholate, the distinct sharp peaks indicate that sodium cholate is present as a crystalline material with characteristic diffraction peaks appearing at angles of $2\theta = (7.57, 8.72, 12.00, 12.99, 13.83, 14.29, 15.13, 16.12, 17.88, 18.64, 35.74, \text{ and } 37.35)$ degrees. The pattern of silybin shows a crystalline material with characteristic diffraction peaks appearing at angles of $2\theta = (13.60, 14.59, 16.05, 17.27, 17.50, 19.63, 20.63, 24.45, 26.28, \text{ and } 26.81)$ degrees. The patterns observed for the mixtures indicate a crystalline mixture of two species. With the increase in w_1 , silybin keeps its crystalline character, but its diffraction intensity is decreased. The position of the diffraction peaks of sodium cholate was not changed, but its strength is increased with the increase in w_1 . This result rules out the possibility of new crystalline phase or a chemical reaction between sodium cholate and silybin in solid state.

Heat Capacity. The specific heat capacities C_p for samples of [sodium cholate (1) + silybin (2)] were measured at temperatures ranging from (303.15 to 370.15) K by DSC. Binary samples with a mass fraction w_1 from (0.100 to 0.900) were prepared by the method as described in the section on Sample Preparation. To eliminate the effect of water, the DSC scan was repeatedly run three times from ambient temperature to 393 K, and then C_p was measured during the fourth run.

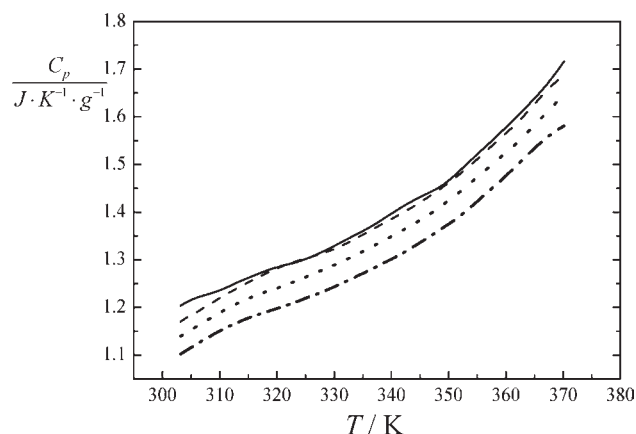
The value of the composition (w_1) was determined in the stage of mixture preparation as described in the section on Sample

Table 1. Heat Capacity, $C_p/J \cdot K^{-1} \cdot g^{-1}$, for Systems of [Sodium Cholate (1) + Silybin (2)] with Mass Fraction w_1

T/K	w_1										
	0	0.100	0.200	0.250	0.333	0.500	0.667	0.750	0.801	0.900	1
303.15	1.20	1.17	1.14	1.1	1.16	1.27	1.33	1.31	1.32	1.34	1.36
304.15	1.21	1.18	1.15	1.11	1.17	1.28	1.33	1.32	1.32	1.34	1.36
305.15	1.22	1.18	1.15	1.12	1.18	1.28	1.34	1.32	1.33	1.35	1.37
306.15	1.22	1.19	1.16	1.12	1.19	1.29	1.35	1.33	1.34	1.35	1.37
307.15	1.23	1.2	1.17	1.13	1.20	1.30	1.35	1.34	1.34	1.36	1.38
308.15	1.23	1.21	1.18	1.14	1.20	1.30	1.36	1.34	1.35	1.37	1.38
309.15	1.23	1.21	1.18	1.15	1.21	1.31	1.36	1.35	1.35	1.37	1.39
310.15	1.24	1.22	1.19	1.15	1.22	1.31	1.37	1.35	1.36	1.38	1.39
311.15	1.24	1.23	1.20	1.16	1.22	1.32	1.37	1.36	1.36	1.38	1.40
312.15	1.25	1.23	1.20	1.16	1.23	1.32	1.38	1.36	1.37	1.38	1.40
313.15	1.25	1.24	1.21	1.17	1.24	1.33	1.38	1.37	1.37	1.39	1.40
314.15	1.26	1.25	1.21	1.17	1.24	1.33	1.38	1.37	1.38	1.39	1.41
315.15	1.26	1.25	1.22	1.18	1.25	1.34	1.39	1.37	1.38	1.4	1.41
316.15	1.27	1.26	1.22	1.18	1.25	1.34	1.39	1.38	1.39	1.4	1.42
317.15	1.27	1.27	1.23	1.19	1.26	1.34	1.4	1.38	1.39	1.41	1.42
318.15	1.28	1.27	1.23	1.19	1.26	1.35	1.4	1.39	1.40	1.41	1.42
319.15	1.28	1.28	1.24	1.19	1.27	1.35	1.4	1.39	1.40	1.41	1.43
320.15	1.28	1.28	1.24	1.2	1.27	1.36	1.41	1.4	1.40	1.42	1.43
321.15	1.29	1.29	1.25	1.2	1.27	1.36	1.41	1.4	1.41	1.42	1.44
322.15	1.29	1.29	1.25	1.21	1.28	1.37	1.42	1.41	1.42	1.43	1.44
323.15	1.29	1.30	1.25	1.21	1.28	1.37	1.42	1.41	1.42	1.43	1.45
324.15	1.30	1.30	1.26	1.22	1.28	1.38	1.43	1.41	1.42	1.44	1.45
325.15	1.30	1.30	1.26	1.22	1.29	1.38	1.43	1.42	1.43	1.44	1.45
326.15	1.31	1.31	1.27	1.22	1.29	1.38	1.43	1.42	1.43	1.45	1.46
327.15	1.31	1.31	1.27	1.23	1.29	1.39	1.44	1.42	1.44	1.45	1.46
328.15	1.32	1.31	1.28	1.23	1.3	1.39	1.44	1.43	1.44	1.45	1.46
329.15	1.32	1.32	1.28	1.24	1.3	1.39	1.45	1.43	1.44	1.45	1.47
330.15	1.33	1.32	1.29	1.24	1.31	1.4	1.45	1.43	1.45	1.46	1.47
331.15	1.34	1.33	1.29	1.25	1.31	1.4	1.45	1.44	1.45	1.46	1.47
332.15	1.34	1.33	1.3	1.25	1.32	1.41	1.46	1.44	1.46	1.47	1.48
333.15	1.35	1.34	1.31	1.26	1.33	1.41	1.46	1.45	1.46	1.47	1.48
334.15	1.36	1.35	1.31	1.27	1.33	1.42	1.47	1.45	1.47	1.47	1.48
335.15	1.36	1.35	1.32	1.27	1.34	1.42	1.47	1.46	1.47	1.48	1.49
336.15	1.37	1.36	1.32	1.28	1.34	1.43	1.48	1.46	1.48	1.48	1.49
337.15	1.38	1.37	1.33	1.28	1.35	1.43	1.48	1.47	1.48	1.49	1.50
338.15	1.38	1.37	1.34	1.29	1.36	1.44	1.48	1.47	1.49	1.49	1.50
339.15	1.39	1.38	1.34	1.30	1.36	1.44	1.49	1.48	1.49	1.50	1.50
340.15	1.4	1.39	1.35	1.3	1.37	1.45	1.49	1.48	1.5	1.5	1.51
341.15	1.41	1.39	1.36	1.31	1.37	1.45	1.5	1.48	1.5	1.51	1.51
342.15	1.41	1.4	1.36	1.31	1.38	1.46	1.5	1.49	1.5	1.51	1.51
343.15	1.42	1.41	1.37	1.32	1.39	1.46	1.51	1.49	1.51	1.51	1.52
344.15	1.43	1.41	1.38	1.33	1.4	1.47	1.51	1.5	1.52	1.52	1.52
345.15	1.43	1.42	1.38	1.34	1.4	1.48	1.52	1.5	1.52	1.52	1.53
346.15	1.44	1.43	1.39	1.35	1.41	1.48	1.53	1.51	1.53	1.53	1.53
347.15	1.44	1.44	1.4	1.35	1.42	1.49	1.53	1.52	1.53	1.53	1.54
348.15	1.45	1.45	1.41	1.36	1.43	1.5	1.54	1.52	1.54	1.54	1.54
349.15	1.46	1.45	1.42	1.37	1.43	1.51	1.55	1.53	1.55	1.54	1.54
350.15	1.47	1.46	1.43	1.38	1.44	1.52	1.55	1.54	1.55	1.55	1.55
351.15	1.48	1.47	1.44	1.39	1.45	1.52	1.56	1.54	1.56	1.56	1.55
352.15	1.49	1.48	1.44	1.39	1.46	1.53	1.57	1.55	1.56	1.56	1.56
353.15	1.5	1.49	1.45	1.4	1.47	1.54	1.57	1.56	1.57	1.57	1.56

Table 1. Continued

T/K	w_1										
	0	0.100	0.200	0.250	0.333	0.500	0.667	0.750	0.801	0.900	1
354.15	1.51	1.5	1.47	1.41	1.48	1.55	1.58	1.56	1.58	1.57	1.56
355.15	1.52	1.51	1.48	1.42	1.49	1.55	1.59	1.57	1.58	1.58	1.57
356.15	1.53	1.52	1.48	1.44	1.5	1.56	1.6	1.58	1.59	1.58	1.57
357.15	1.54	1.54	1.5	1.45	1.51	1.57	1.6	1.59	1.6	1.59	1.58
358.15	1.56	1.55	1.51	1.46	1.52	1.58	1.61	1.6	1.6	1.59	1.58
359.15	1.57	1.56	1.52	1.47	1.53	1.59	1.62	1.6	1.61	1.6	1.59
360.15	1.58	1.57	1.53	1.48	1.54	1.6	1.63	1.61	1.61	1.6	1.59
361.15	1.59	1.58	1.54	1.49	1.55	1.61	1.64	1.62	1.62	1.61	1.59
362.15	1.6	1.59	1.55	1.5	1.56	1.62	1.64	1.63	1.63	1.61	1.6
363.15	1.62	1.6	1.56	1.51	1.58	1.62	1.65	1.63	1.63	1.62	1.6
364.15	1.63	1.62	1.57	1.52	1.59	1.63	1.66	1.64	1.64	1.62	1.61
365.15	1.64	1.63	1.58	1.54	1.6	1.64	1.66	1.65	1.64	1.63	1.61
366.15	1.65	1.64	1.6	1.55	1.61	1.65	1.67	1.66	1.65	1.63	1.62
367.15	1.67	1.66	1.61	1.56	1.62	1.66	1.68	1.67	1.66	1.64	1.62
368.15	1.68	1.67	1.62	1.56	1.63	1.68	1.69	1.68	1.66	1.64	1.63
369.15	1.7	1.68	1.63	1.57	1.64	1.69	1.7	1.69	1.67	1.65	1.63
370.15	1.72	1.69	1.65	1.58	1.64	1.7	1.71	1.7	1.68	1.65	1.63

**Figure 6.** Curves of C_p against temperature T for [sodium cholate (1) + silybin (2)] with mass fractions of $w_1 = (0, \text{solid line}; 0.100, \text{dashed line}; 0.200, \text{dotted line}; 0.250, \text{dash-dotted line})$, in order from top to bottom.

Preparation. As noted above, during the process of weighing and loading the samples into the DSC crucible, moisture absorption by sample is unavoidable. Therefore, three of the DSC scans were run under the protection of nitrogen to remove moisture. Over the processes of DSC operation, the mass ratio of silybin to sodium cholate was not changed. Only water and solvent were absorbed and/or evaporated. Therefore, the initial value of the composition determined in the section on Sample Preparation is still the better choice for determining composition.

The data of C_p are listed in Table 1. In the range of $w_1 < 0.25$, the trend of C_p with temperature T and w_1 is shown in Figure 6. At a given composition w_1 , the C_p increase with temperature increase, and at a given temperature T , they move downward with the w_1 increase. In the range of $w_1 > 0.333$, the trend of C_p with T and w_1 cannot be distinguished clearly. They overlap to some extent. Instead, they can be distinguished in an alternative

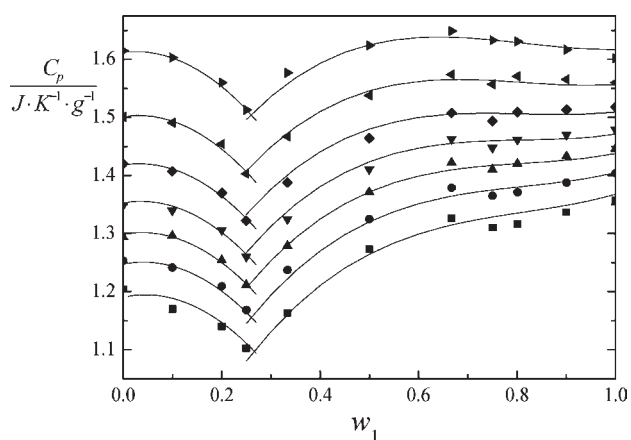


Figure 7. Effect of composition on heat capacity for [sodium cholate (1) + silybin (2)] at temperatures $T = \blacksquare$, 303.15; \bullet , 313.15; \blacktriangle , 323.15; \blacktriangledown , 333.15; \blacklozenge , 343.15; left-pointing triangle, 353.15, and right-pointing triangle, 363.15 K. The fitting curves are shown as lines.

Table 2. Coefficients of eqs 2, 7, and 8, the Standard Uncertainties s , and the Correlation Coefficients R Obtained by Fitting Experimental Data in Two Composition Regions, ($w_1 < 0.250$ and $w_1 > 0.250$), Respectively

$w_1: (0 \text{ to } 0.250)$						
R	0.9992	s	0.0063			
a_{11}	1.1900	a_{12}	0.1790	a_{13}		-1.984
a_{21}	0.4138	a_{22}	-0.08607			
a_3	-0.2883					
a_4	0.3933					
$w_1: (0.250 \text{ to } 1)$						
R	0.9962	s	0.01			
a_{11}	0.6795	a_{12}	2.161	a_{13}	-2.493	a_{14} 1.020
a_{21}	0.5234	a_{22}	-0.2486			
a_3	-0.1975					
a_4	0.2252					

way. Figure 7 shows the effect of w_1 on C_p at several constant temperatures. In the region of $w_1 < 0.250$, the C_p decreases with an increase in sodium cholate. After a minimum at about $w_1 = 0.250$, in the region of $w_1 > 0.250$, the C_p increases with the increase in w_1 . The minimum, $w_1 = 0.250$, looks as if it was a "eutectic" composition.

Fitting Experimental C_p . There are many empirical equations to correlate the C_p with temperature.^{14,15} For example, the dependence of C_p on temperature can be expressed by eq 2 in the range from an initial temperature T_i to a final temperature T_f .

$$C_p / (\text{J} \cdot \text{K}^{-1} \cdot \text{g}^{-1}) = a_1 + a_2x + a_3x^2 + a_4x^3 \quad (2)$$

where

$$x = (T - T_i) / (T_f - T_i) \quad (3)$$

and a_i is the coefficient of the polynomial equation. For a binary system, coefficient a_i depends on the composition w_1 to some extent. For example, a_1 is relative to the mixing effect of two components at temperature T_i . a_2 is a coefficient of the linear

relationship between C_p and temperature, which is relative to the composition too.

Inspecting the curves in Figure 7, it is observed that they have similar shapes at different temperatures, and a minimum is present in all cases. The minima separate the solid mixture into two parts. One is the system of sodium cholate dispersed in silybin at $w_1 < 0.25$, and another is the system of silybin dispersed in sodium cholate at $w_1 > 0.25$. An essential step to fit the data of C_p is how to express the mixing behavior at T_i .

For a binary system at constant temperature T , the thermodynamic properties, for example C_p , can be expressed as eq 4.

$$C_p = w_1 C_{p1}^* + w_2 C_{p2}^* + C_p^{\text{ex}} \quad (4)$$

where C_{pi}^* is the heat capacity of component i , C_p^{ex} is the excess/ or mixing heat capacity, and this is usually expressed as a virial function.^{17,18}

$$C_p^{\text{ex}} = c_{ii}w_i^2 + c_{iii}w_i^3 + \dots \quad (5)$$

where the coefficient c_{ii} and c_{iii} represent, at least notionally, the interactions occurring between the subscripted species (i) in the medium considered. If component 1 is specified as the solute and 2 as the medium, just as in the case of $w_1 < 0.25$, using eqs 4 and 5, we have

$$C_p = C_{p2}^* + (C_{p1}^* - C_{p2}^*)w_1 + c_{11}w_1^2 + c_{111}w_1^3 + \dots \quad (6)$$

It means that the C_p of the binary mixture can be expressed by a polynomial equation with concentration w_1 as a variable. If the position of 1 and 2 are exchanged, just as in the case of $w_1 > 0.25$, that silybin (2) is treated as solute and sodium cholate (1) as the medium, the formula can still be applicable.

The physical meaning of coefficients a_1 in eq 2 is the C_p at T_i . Applying eq 6 to a binary system, a_1 can be simply expressed by

$$a_1 = a_{11} + a_{12}w_1 + a_{13}w_1^2 + a_{14}w_1^3 \quad (7)$$

where a_{12} and a_{13} are of the physical meaning of virial coefficients. Using eq 7 to fit experimental data, the composition region should be specified, that is, to specify which component is the medium. In this work, eq 7 is used in two concentration regions, $w_1 < 0.25$ and $w_1 > 0.25$, respectively.

The coefficients a_2 , a_3 , and a_4 in eq 2 express the temperature effect on C_p . It was found from Figure 7 that the temperature effect on the curve shape of C_p versus w_1 , the relationship between C_p and w_1 , is not complex and is not in confusion. This observation suggests that the effect of composition on a_2 can be expressed by a linear function.

$$a_2 = a_{21} + a_{22}w_1 \quad (8)$$

and the effect of composition on a_3 and a_4 is negligible.

Combining eqs 2, 3, 7, and 8, the data of C_p were fitted in the temperature range from T_i to T_f and in two composition regions, $w_1 < 0.25$ and $w_1 > 0.25$, respectively, to meet the requirements of the virial equation. The fitting result is given in Table 2 and graphically shown in Figure 7. In the region of $w_1 < 0.250$, a quadratic equation for a_1 works fine, whereas in the region of $w_1 > 0.250$, a cubic equation is a better choice. The correlation coefficient R and standard uncertainty s of the fits in two composition regions are given in Table 2, respectively.

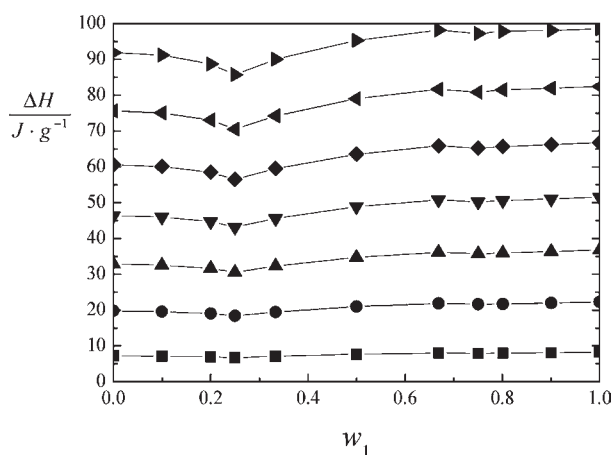


Figure 8. Changes of enthalpy against mass fraction w_1 for the system of [sodium cholate (1) + silybin (2)] at temperature $T = \blacksquare$, 308.15; \bullet , 318.15; \blacktriangle , 328.15; \blacktriangledown , 338.15; \blacklozenge , 348.15; left-pointing triangle, 358.15, and right-pointing triangle, 368.15 K.

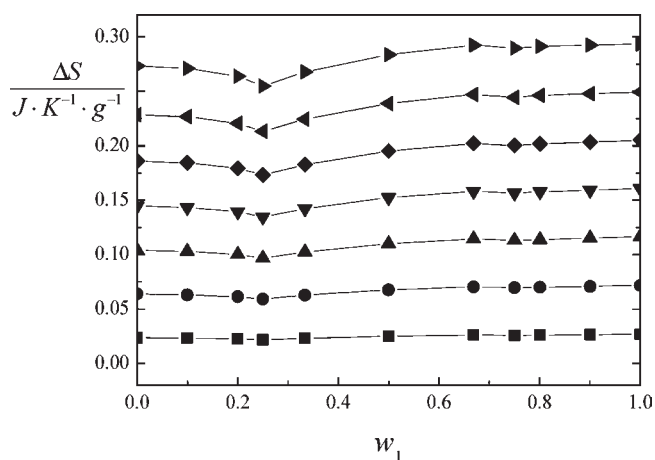


Figure 9. Changes of entropy against mass fraction w_1 for system of [sodium cholate (1) + silybin (2)] at temperature $T = \blacksquare$, 308.15; \bullet , 318.15; \blacktriangle , 328.15; \blacktriangledown , 338.15; \blacklozenge , 348.15; left-pointing triangle, 358.15, and right-pointing triangle, 368.15 K.

THERMODYNAMIC PROPERTIES

The change in thermodynamic properties, from the initial temperature T_i to a given temperature T , can be calculated from the C_p data. Thermodynamic relations are given as below.

$$\Delta H = \int_{T_i}^T C_p dT \quad (9)$$

$$\Delta S = \int_{T_i}^T (C_p/T) dT \quad (10)$$

$$\Delta G = \Delta H - T\Delta S \quad (11)$$

where H , S , and G are the enthalpy, entropy, and Gibbs function, respectively. To see the effect of mixing on ΔH and ΔS clearly, the curves of ΔH and ΔS against w_1 at several constant temperatures, $T = (308.15, 318.15, 328.15, 338.15, 348.15, 358.15, \text{ and } 368.15) \text{ K}$, are shown in Figures 8 and 9, respectively.

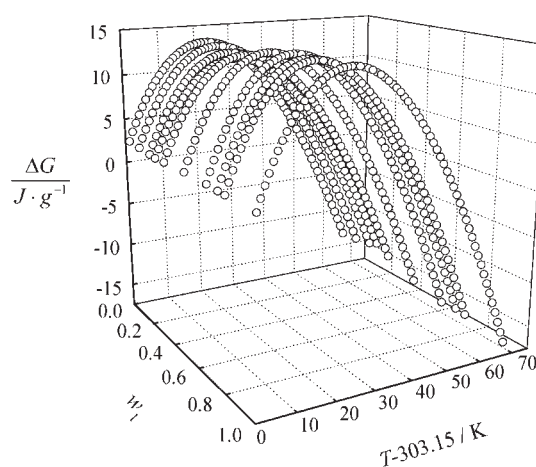


Figure 10. 3D curves of the changes of Gibbs function (ΔG) of [sodium cholate (1) + silybin (2)] against temperature T and mass fraction w_1 .

Apparently, the curves in Figures 8 and 9 have similar trends to those in Figure 7. In Figure 10, the 3D curve of ΔG against w_1 and T are shown. It shows that, with an increase in temperature T , ΔG increases first and then decreases. This means that, at the higher temperature region, the contribution of entropy becomes appreciable.

CONCLUSION

The heat capacity C_p of a solid mixture of [sodium cholate (1) + silybin (2)] is an essential piece of data in predicting the thermodynamic properties and the phase state. From the curves of C_p against w_1 at constant temperature, it appears that the solid state of this binary system is a mixture of two crystalline solids with a "minimum" at $w_1 = 0.250$. In aqueous solution, sodium cholate has other special properties, such as aggregation and alkalinity. However, in the solid state, special interactions between sodium cholate and silybin are not observable. By using empirical equations, the relationship of C_p and T within two concentration regions, $w_1 < 0.25$ and $w_1 > 0.25$, was fitted, respectively.

AUTHOR INFORMATION

Corresponding Author

*E-mail: tcbai@suda.edu.cn. Tel.: +(86)51265880363. Fax: +(86)51265880089.

Funding Sources

This project was funded by the Priority Academic Program Development of Jiangsu Higher Education Institutions.

REFERENCES

- (1) Flora, K.; Hahn, M.; Rosen, H.; Benner, K. Milk Thistle (*Silybum Marianum*) for the Therapy of Liver Disease. *Am. J. Gastroenterol.* **1998**, *93*, 139–143.
- (2) Škottová, N.; Krečman, V. Silymarin as a Potential Hypocholesterolaemic Drug. *Physiol. Res.* **1998**, *47*, 1–7.
- (3) Lee, D. Y. W.; Liu, Y. Molecular Structure and Stereochemistry of Silybin A, Silybin B, Isosilybin A, and Isosilybin B, Isolated from *Silybum Marianum* (Milk Thistle). *J. Nat. Prod.* **2003**, *66*, 1171–1174.
- (4) El-Samalgly, M. S.; Affi, N. N.; Mahmoud, E. A. Increasing Bioavailability of Silymarin Using a Buccal Liposomal Delivery System: Preparation and Experimental Design Investigation. *Int. J. Pharm.* **2006**, *308*, 140–148.

(5) Han, W.; Bai, T. C.; Zhu, J. J. Thermodynamic Properties for the Solid-Liquid Phase Transition of Silybin + Poloxamer 188. *J. Chem. Eng. Data* **2009**, *54*, 1889–1893.

(6) Yu, J.-N.; Zhu, Y.; Wang, L.; Peng, M.; Tong, S. S.; Cao, X.; Qiu, H.; Xu, X. M. Enhancement of Oral Bioavailability of the Poorly Water-Soluble Drug Silybin by Sodium Cholate/Phospholipid-Mixed Micelles. *Acta Pharmacol. Sin.* **2010**, *31*, 759–764.

(7) Guo, J.; Wu, T.; Ping, Q.; Chen, Y.; Shen, J.; Jiang, G. Solubilization and Pharmacokinetic Behaviors of Sodium Cholate/Lecithin-Mixed Micelles Containing Cyclosporine A. *Drug Delivery* **2005**, *12*, 35–39.

(8) Westergaard, H.; Dietschy, J. M. The Mechanism whereby Bile Acid Micelles Increase the Rate of Fatty Acid and Cholesterol Uptake into the Intestinal Mucosal Cell. *J. Clin. Invest.* **1976**, *58*, 97–108.

(9) Matsuoka, K.; Kuranaga, Y.; Moroi, Y. Solubilization of Cholesterol and Polycyclic Aromatic Compounds into Sodium Bile Salt Micelles (Part 2). *Biochim. Biophys. Acta* **2002**, *1580*, 200–214.

(10) Sugioka, H.; Moroi, Y. Micelle Formation of Sodium Cholate and Solubilization into the Micelle. *Biochim. Biophys. Acta* **1998**, *1394*, 99–110.

(11) Blagden, N.; de Matas, M.; Gavan, P. T.; York, P. Crystal Engineering of Active Pharmaceutical Ingredients to Improve Solubility and Dissolution Rates. *Adv. Drug Delivery Rev.* **2007**, *59*, 617–630.

(12) Liu, Z. H. *Introduction to Thermal Analysis*; Chemical Industry Press: Beijing, 1991.

(13) Tong, B.; Tan, Z. C.; Shi, Q.; Li, Y. S.; Yue, D. T.; Wang, S. X. Thermodynamic Investigation of Several Natural Polyols (I): Heat Capacities and Thermodynamic Properties of Xylitol. *Thermochim. Acta* **2007**, *457*, 20–26.

(14) Hua, X.; Kaplan, D.; Cebe, P. Effect of Water on the Thermal Properties of Silk Fibroin. *Thermochim. Acta* **2007**, *461*, 137–144.

(15) Xu, K.; Song, J.; Zhao, F.; Ma, H.; Gao, H.; Chang, C.; Ren, Y.; Hu., R. Thermal Behavior, Specific Heat Capacity and Adiabatic Time-to-Explosion of G(FOX-7). *J. Hazard. Mater.* **2008**, *158*, 333–339.

(16) Xie, J. X.; Chang, J. B.; Wang, X. M. *Infrared Spectroscopy Application in Organic Chemistry and Drug Chemistry*; Science Press: Beijing, 2001.

(17) Jones, M. N. *Biochemical Thermodynamics*, 2nd ed.; Elsevier: New York, 1988.

(18) Wood, R. H.; Lilley, T. H.; Thompson, P. T. Rapidly Converging Activity Expansions for Representing the Thermodynamic Properties of Fluid Systems: Gases, Non-electrolyte Solutions, Weak and Strong Electrolyte Solutions. *J. Chem. Soc., Faraday Trans. 1* **1978**, *74*, 1301–1323.